Supplementary Information

Sponge network-shaped Mn_3O_4/C anode derived from a simple, one-pot metal organic framework-combustion technique for improved lithium ion storage

Balaji Sambandam,‡ Vaiyapuri Soundharrajan,‡ Vinod Mathew, Jinju Song, Sungjin Kim, Jeonggeun Jo, Duong Pham Tung, Seokhun Kim and Jaekook Kim*

Department of Materials Science and Engineering, Chonnam National University, Gwangju 500-757, South Korea.

*E-mail: jaekook@chonnam.ac.kr

‡These authors contributed equally to this work.

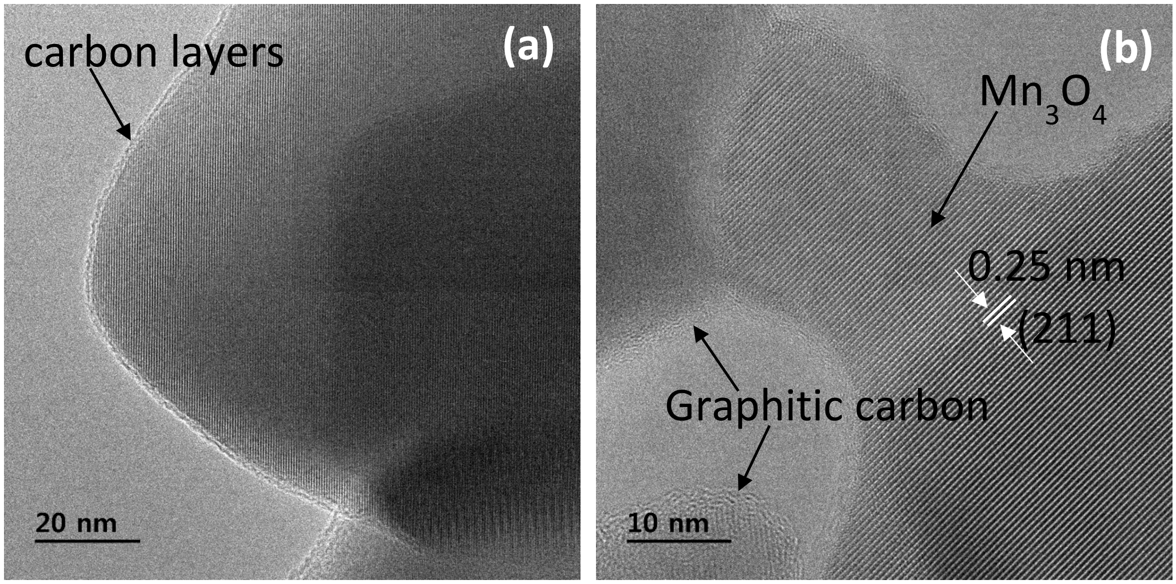

Fig. S1. HR-TEM images of Mn_3O_4 (a) low magnification; (b) high magnification shows distinguished lattice fringes from the surface carbon to the core

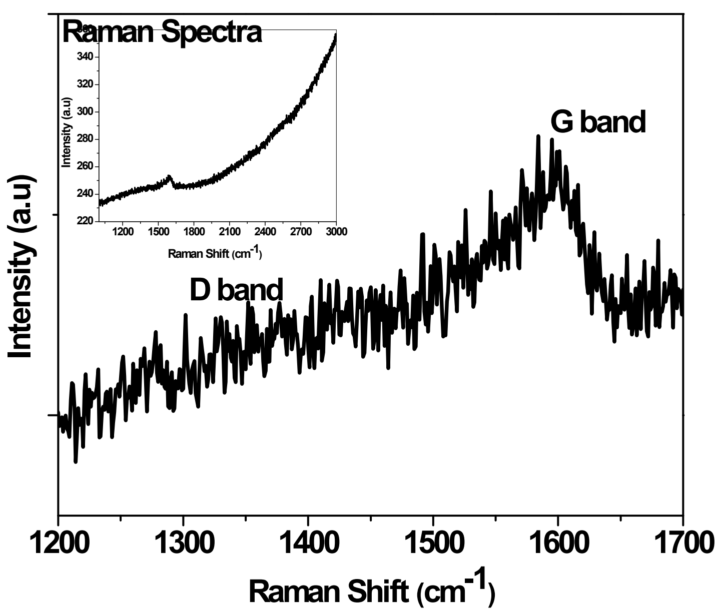

Fig. S2. Raman spectra for Mn_3O_4/C at a frequency region of 1200-1700 cm^{-1}; inset: extended region to 3000 cm^{-1}.

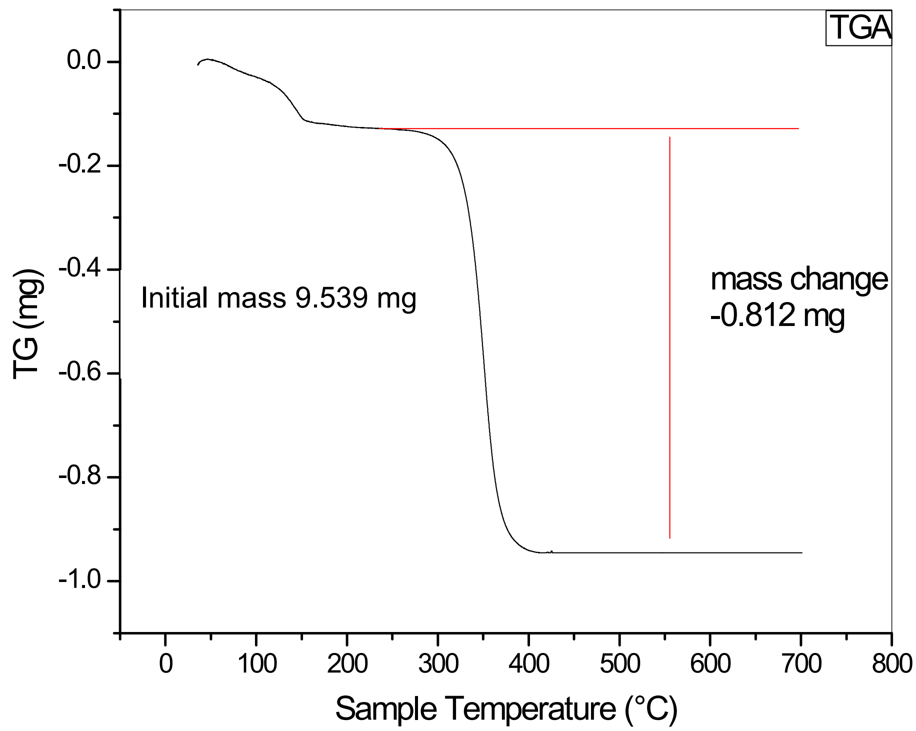

Fig. S3 TGA analysis for Mn_3O_4/C

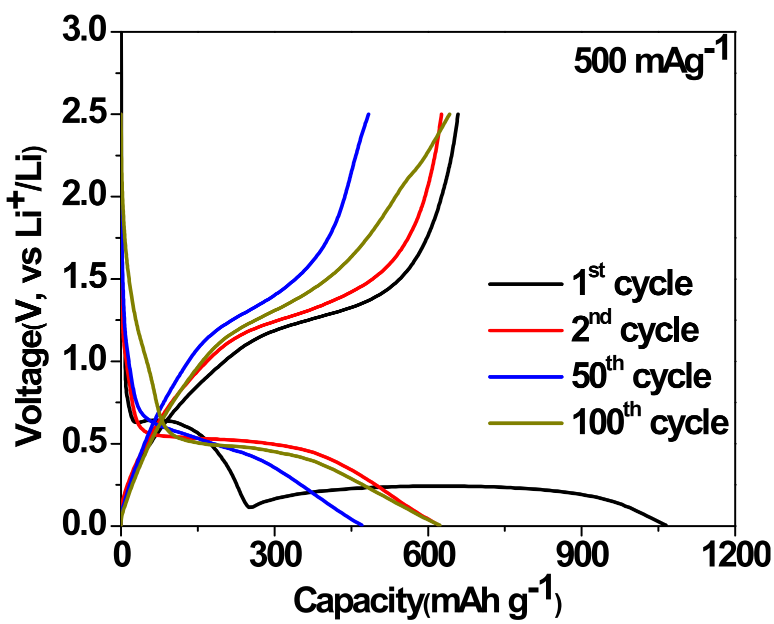

Fig. S4. Selected charge/discharge profiles at a current density 500 mA g^{-1}

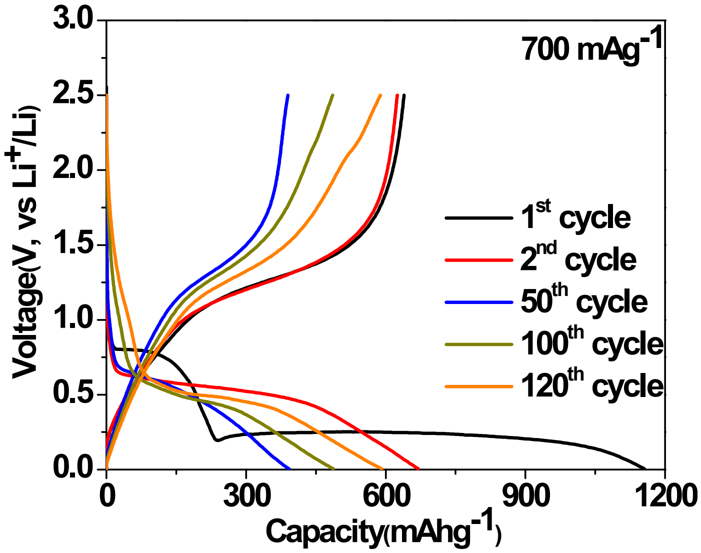

Fig. S5. Selected charge/discharge profiles at a current density 700 mA g^{-1}

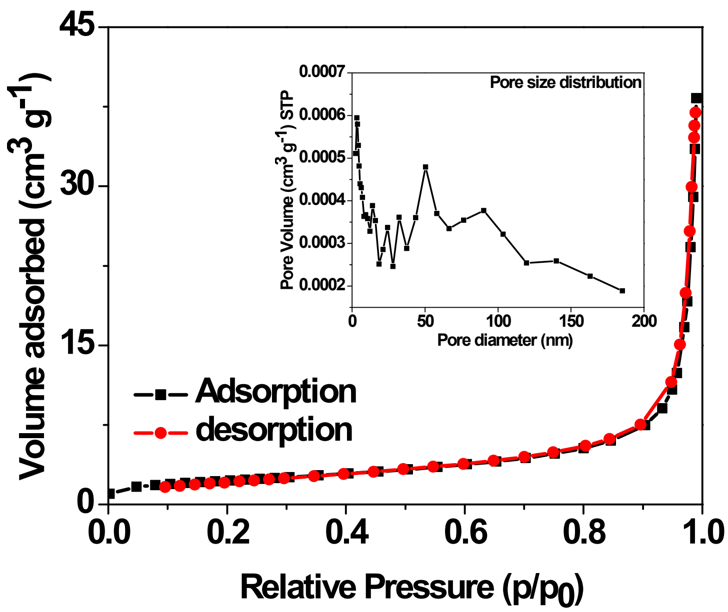

Fig. S6. BET surface area profile of adsorption/desorption isotherm curve. Inset: pore size distribution for Mn_3O_4 with sponge network morphology

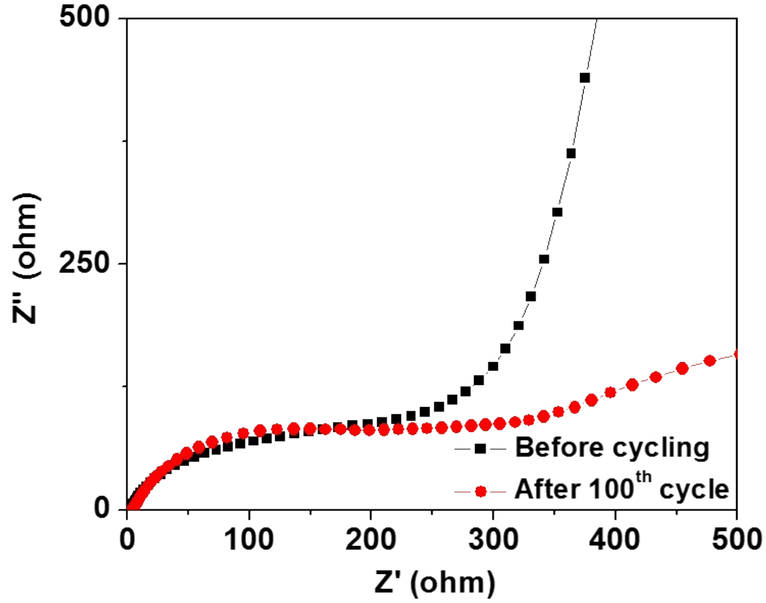

Fig. S7. EIS measurements before and after cycling at 200 mA g^{-1} current density

Table S1. Morphology dependent electrochemical performance for Mn_3O_4 anode synthesized by different techniques.

s.no	materials/morphology	current density mA g^{-1}	cycles	discharge capacity; capacity retention mAh g^{-1}; CE%	rate capability (mAh g^{-1}) at current density (mA g^{-1})	potential window (V)	Ref.
1	Mn_3O_4/C sponge network	200 500 700	100 120 120	1185/1st cycle; 770/100th cycle; 100%/100th cycle 1065/1st cycle; 651/120th cycle; 97.6%/100th cycle 1155/1st cycle; ~591/120th cycle; 100%/120th cycle	~150 at 10000	0.005 to 2.5	This work
2	Highly Flexible Graphene/Mn_3O_4 Nanocomposite Membrane	100	100	1271/1st cycle; 802/100th cycle; ~99%/100th cycle	308 at 2000	0.005 to 3.0	SR1
3	Mn_3O_4 octahedra	100 300	500 500	918/1st cycle; 746/500th cycle; 81.3%/500th cycle 807/1st cycle; 628/500th cycle; 77.8%/500th cycle	240 at 1500	0.005 to 3.0	SR2
4	Mn_3O_4 Nanorods	0.1 C (<100 mA g^{-1})	100	1050/1st cycle; 108/100th cycle; 10.3%/100th cycle	---	0.005 to 3.0	. SR3

5	Order-aligned Mn_3O_4 nanostructure	940 20 C 40 C	100 100 100	919/1st cycle; 882/85th cycle; 96.0%/85th cycle; 637/100th cycle; 494/100th cycle;	550 at 32 C	0.01 to 3.0	SR4
5	Mesoporous stacked Mn_3O_4 nanosheets	0.1 C (<100 mA g^{-1})	60	824/1st cycle; 400/60th cycle;	298 at 1.5 C	0.01 to 3.0	SR4
7	Mn_3O_4 Fibers	0.5 mA cm^{-2} (~208 mA g^{-1})	50	860/1st cycle; 450/50th cycle; 52.3%/50th cycle	--	0.01 to 3.0	SR6
8	Mn_3O_4 -spongelike nanostructure	30	40	1327/1st cycle; ~800/40th cycle; 60.3%/40th cycle	~500 at 10C	0.01 to 3.0	SR7
9	Mn_3O_4 NPs Mn_3O_4 NPs-Graphene Hybrid	40	100	300/1st cycle; 115/100th cycle; 38.3%/10th cycle ~900/1st cycle	----- 390 at 1600	0.01 to 3.0	SR8
10	Mn_3O_4 /VGCF Composite	100/200 500	120 200	>1200/1st cycle (100 mA g^{-1}); >1350/120th cycle (200 mA g^{-1}) 855/1st cycle; 1391/200th cycle;	390 at 5000	0.01 to 3.0	SR9
11	Mn_3O_4 tetragonal bipyramids	0.2 C	56	1141/1st cycle; 822/56th cycle; 100%/56th cycle;	471 at 2C	0.01 to 3.0	SR10

12	Mn_3O_4 -coated carbon nanofibers on copper foam	100 5C		1172/1st cycle; > 1100/ 100th cycle 300/100th cycle	391 at 5C	0.01 to 3.0	SR11
13	Carbon quantum dot coated Mn_3O_4	100	50/100	1125/ 1st cycle; 791/100th cycle; 99%/100th cycle	304 at 1000	0.01 to 3.0	SR12
14	Mn_3O_4 /graphene composites	60	40	~1600/1st cycle; >500/ 40th cycle	~200 at 1500	0.01 to 3.0	SR13
15	Mn_3O_4 nanocrystals on reduced graphene oxide	100 1200	10 500	1912/1st cycle; 1198/10th cycle; 95.2%/10th cycle 370/1st cycle; 330/ 500th cycle;	180 at 2000	0.01 to 3.0	SR14
16	Mn_3O_4 @C core–shell	500	100	1525/1st cycle; 765/100th cycle;	380 at 2000	0.01 to 3.0	SR15
17	Carbon Layer Coated Mn_3O_4 Nanorod	40	50	974/1st cycle; 550 /50th cycle; >98%/50th cycle	--	0.01 to 3.0	SR16
18	Mn_3O_4 hollow spheres	200	140	1609/1st cycle; 980/140th cycle; 100%/140th cycle	~300 at 10000	0.01 to 3.0	SR17

19	Porous Mn_3O_4 nanorod/reduced graphene oxide hybrid paper	100	100	943/1st cycle; 573/100th cycle; 100%/100th cycle	196 at 2000	0.005 to 3.0	SR18
20	Mn_3O_4 / graphene composites	60	100	897/1st cycle; ~500/100th cycle;	220 at 750	0.005 to 3.0	SR19
21	Mn_3O_4 nanosheet on graphene via forming a 2D–2D nanostructure	50	50	1890/1st cycle; 1180/50th cycle;	637 at 1000	0.01 to 3.0	SR20
22	Mn_3O_4 –graphene nanocomposite	40	50	1354/1st cycle; ~900/50th cycle; 100%/100th cycle	400 at 2000	0.1 to 3.0	SR21
23	Single crystalline Mn_3O_4 nano-octahedra	50	50	1504/1st cycle; 500/50th cycle; 100%/50th cycle;	350 at 500	0.1 to 3.0	SR22
24	Mn_3O_4 nanocrystals anchored on multi-walled carbon nanotubes	100	50	1380/1st cycle; 592/50th cycle; 63%/50th cycle	387 at 1000	0.1 to 3.0	SR23
25	Mn_3O_4 -GN composite aerogels	50	60	1132/1st cycle; 665/60th cycle; 97.7%/60th cycle	-----	0.1 to 3.0	SR24
26	Mn_3O_4 Nanoparticles on Nitrogen-doped Graphene	200	40	1275/1st cycle; 800/40th cycle;	382 at 2000	0.1 to 3.0	SR25

1C = 946 mAh g^{-1}

References

SR1. Q. Hao, J. Wang and C. Xu, *J. Mater. Chem. A,* 2, **2014**, 87–93.

SR2. J. G. Wang, D. Jin, R. Zhou, X. Li, X. Liu, C. Shen, K. Xie, B. Li, F. Kang, B. Wei, ACS Nano, **2016**, DOI: 10.1021/acsnano.6b02319.

SR3. X. Shen, Z. Ji, H. Miao, J. Yang and K. Chen, *J. Alloys Compd.*, 509, **2011**, 5672–5676.

SR4. J. Wang, N. Du, H. Wu, H. Zhang, J. Yu and D. Yang, *J. Power Sources,* 222, **2013**, 32–37.

SR5. D. P. Dubal and R. Holze, *RSC Adv.*, 2, **2012**, 12096-12100.

SR6. Q. Fan and M. S. Whittingham, Electrochem.Solid-State Lett., 10, **2007**, A48-A51.

SR7. J. Gao, M. A. Lowe and H. D. Abruna, *Chem. Mater.*, 23, **2011**, 3223–3227.

SR8. H. Wang, L. Cui, Y. Yang, H. S. Casalongue, J. T. Robinson, Y. Liang, Y. Cui, H. Dai, *J. Am. Chem. Soc.,* 132, **2010**, 13978–13980.

SR9. F. Ma, A. Yuan and J. Xu, *ACS Appl. Mater. Interfaces*, 6, **2014**, 18129−18138.

SR10. T. Li, C. Guo, B. Sun, T. Li, Y. Li, L. Hou and Y. Wei, *J. Mater. Chem. A*, 3, **2015**, 7248–7254.

SR11. H. Yue, F. Li, Z. Yang, X. Li, S. Lin and D. He, *J. Mater. Chem. A*, 2, **2014**, 17352–17358.

SR12. M. Jing, J. Wang, H. Hou, Y. Yang, Y. Zhang, C. Pan, J. Chen, Y. Zhu and X. Ji, *J. Mater. Chem. A*, 3, **2015**, 16824-16830.

SR13. I. Nam, N.D. Kim, G. Kim, J. Park and J. Yi, *J. Power Sources*, 244, **2013**, 56-62.

SR14. H. Huang, L. Zhang, Y. Xia, Y. Gan, X. Tao, C. Liang and W. Zhang, *New J. Chem.*, 38, **2014**, 4743—4747.

SR15. X. Ma, Y. Zhai, N. Wang, J. Yang and Y. Qian, *RSC Adv.*, 5, **2015**, 46829-46833.

SR16. G. Jian, Y. Xu, L. Lai, C. Wang and M. R. Zachariah, *J. Mater. Chem. A,* 2, **2014**, 4627–4632.

SR17. C. Wang, L. Yin, D. Xiang and Y. Qi, *ACS Appl. Mater. Interfaces*, 4, **2012**, 1636−1642.

SR18. S.K. Park, C.Y. Seong, S. Yoo and Y. Piao, *Energy*, 99, **2016**, 266-273.

SR19. Y. Ren, J. Wang, X. Huang, B. Yang and J. Ding, *RSC Adv.*, 5, **2015**, 59208–59217.

SR20. Y. Zhao, G. Chen, C. Yan, C. Lv, R. Wang and J. Sun, *RSC Adv.*, 5, **2015**, 106206-106212.

SR21. L. Li, Z. Guo, A. Du and H. Liu, *J. Mater. Chem.*, 22, **2012**, 3600–3605.

SR22. S. Z. Huang, J. Jin, Y. Cai, Y. Li, H. Y. Tan, H. E. Wang, G. Van Tendeloo, B. L. Su, *Nanoscale*, 6, **2014**, 6819–6827.

SR23. Z. H. Wang, L. X. Yuan, Q. G. Shao, F. Huang, Y. H. Huang, *Mater. Lett.*, 80, **2012**, 110–113.

SR24. H. Tang, Y. Sui, X. Zhu and Z. Bao, *Nanoscale Res. Lett.*, 10, **2015**, 260.

SR25. S. K. Park, A. Jin, S. H. Yu, J. Ha, B. Jang, S. Bong, S. Woo, Y. E. Sung and Y. Piao, *Electrochim. Acta*, 120, **2014**, 452–459.